



Cite this: DOI: 10.1039/d5fb00841g

## Enhancing functional and structural properties of chia seed flour through combined pH shifting and high-speed homogenization

Divyang Solanki, <sup>a</sup> Bhesh Bhandari, <sup>a</sup> Pratheep K. Annamalai, <sup>a</sup> Jatindra K. Sahu <sup>b</sup> and Sangeeta Prakash <sup>\*a</sup>

Chia seed flour (CSF) is valued for its nutritional richness and functional attributes; however, its dark colour, high water absorption, and viscosity limit its application in leavened and other processed foods. This study explored the combined use of alkaline pH shifting (pH 8, 10, and 12) and high-speed homogenization (HSH) to improve the techno-functional properties of raw chia seed flour (RCF). The process yielded modified flours (pH 8CF, pH 10CF, and pH 12CF) and residues, which were compared with untreated controls. The results showed that flour yield significantly increased with higher pH, with pH 12CF reaching ~75%. Colour improved under HSH and pH 8 treatment, while particle size was reduced, creating more homogeneous dispersions. Solubility increased markedly (35–45% in modified samples, and 22% in RCF), and zeta potential became more negative, suggesting enhanced colloidal stability. Water-holding and swelling capacities declined, but oil-holding capacity increased, reflecting altered interactions between fibre and protein. Rheological analysis revealed a drastic reduction in viscosity (up to 900 times lower), alleviating the processing limitations of RCF in bakery systems. FTIR and DSC analyses confirmed molecular rearrangements of proteins, polysaccharides, and lipids. Overall, pH–HSH treatment offers a cost-effective and scalable approach to produce lighter, low-viscosity chia flours with improved functionality for bakery, gluten-free, and plant-based product development.

Received 31st October 2025  
Accepted 18th December 2025

DOI: 10.1039/d5fb00841g  
[rsc.li/susfoodtech](http://rsc.li/susfoodtech)

### Sustainability spotlight

This research developed a sustainable approach to enhance the functionality of chia seed flour (CSF), a nutrient-rich but underutilised ingredient due to its dark colour and high viscosity. By applying combined alkaline pH shifting and high-speed homogenization (pH–HSH), the study produced lighter, low-viscosity chia flours with improved solubility, stability, and processing potential. The modified flours demonstrated greater suitability for bakery, gluten-free, and plant-based applications, offering a cost-effective, scalable method to expand the use of chia in diverse food systems. This innovation supports value-added utilisation of natural resources, reducing waste and promoting sustainable ingredient development within the food industry.

## 1 Introduction

Chia seeds (CSs) serve as a potential solution for addressing global food insecurity, providing multiple pieces of evidence on their health and nutritional benefits.<sup>1</sup> Previous research defines chia seeds as a “forgotten seed” with good nutritional<sup>2</sup> and phytochemical profiles.<sup>3,4</sup> The utilisation of CS and raw chia seed flour (RCF) in various products is also well-documented.<sup>5</sup> RCF is added to foods mainly because of its health properties, and functional properties such as emulsifying activity, gelling capacity, and water/fat binding capacity, which result in technological benefits along with processing.<sup>6</sup> Recent reports have

mentioned the use of CS ingredients for the creation of meat analogs because of their diverse technological properties.<sup>7</sup>

However, RCF has limited use in bread as it reduces the total score during sensory analysis and specific volumes of loaves.<sup>8</sup> However, using CS or RCF has increased consumers' high levels of acceptability and purchase plans due to the higher content of polyunsaturated fat, mainly omega-3 fatty acids. Adding hydrogenated vegetable fat was preferred to reduce the severe impact of whole RCF on the pound cake.<sup>9</sup> Similarly, the use of RCF in pasta reduced the lightness of the product<sup>10</sup> and results in darker pasta upon addition of chia seed-based ingredients (chia fibre and chia proteins), which may negatively affect consumer preference. However, the higher fibre and protein content in these products can be viewed positively by many consumers. In pasta, chia fibre and chia protein exhibit more functional properties than RCF, suggesting a potential modification of chia seed flour.

<sup>a</sup>School of Agriculture and Food Sustainability, The University of Queensland, Brisbane, QLD, 4072, Australia. E-mail: [s.prakash@uq.edu.au](mailto:s.prakash@uq.edu.au)

<sup>b</sup>Food Customization Research Lab, Centre for Rural Development and Technology, Indian Institute of Technology Delhi, New Delhi, 110 016, India



However, very limited research has been conducted on the fractions of chia seed and RCF to understand their functional properties. The gelling properties of intact RCF were studied by Ramos *et al.*,<sup>11</sup> which explained the improved gelling, textural, and rheological properties of RCF at 130 g kg<sup>-1</sup> at 90 °C for 30 min. To steer the wide range of functional properties of chia seed flour (partially defatted chia fibre–protein concentrate) in the leavened bakery products,<sup>12</sup> high-pressure homogenization treatments were explored, altering the particle size, water-holding and oil-holding capacity, solubility, and soluble dietary fibre content. The study confirms an improvement in the solubility of partially defatted chia fibre–protein concentrate, along with an increase in the conversion of insoluble fibres to soluble fibres.

Thus, this proposed study utilised RCF and modified its functional properties by adjusting the pH and employing high-speed homogenization (HSH). Literature studies on the impact of different pH levels on the extraction of protein isolates from buckwheat<sup>13</sup> and chia seed<sup>14,15</sup> also reported a positive impact on functional properties. For the preparation of chia seed protein isolates, pH levels of 8, 10, and 12 were selected, and their significant influence on the functional properties of chia seed protein isolates was confirmed.<sup>15</sup> Defatted and demucilaged chia seed flour was subjected to pH shifting (pH 8.5, 10, and 12) to isolate chia seed proteins, demonstrating improvement in the functional and bio-functional properties.<sup>16</sup> The impact of pH shifting on various other plant-based matrices is well-documented, which supports our hypothesis that pH shifting helps modify the structural and functional properties of chia seed proteins and carbohydrates. However, to date, no study has examined the combined effect of pH-shifting and high-speed homogenization on intact chia seed flour, a gap this research seeks to address.

High-speed homogenization (HSH) is usually used to prepare foams, emulsions, and suspensions. During processing, the medium is drawn axially into the gap between the rotor and stator, where the sample particles are ground under strong shear and thrust forces generated at high rotation speeds (10 000–20 000 rpm).<sup>17</sup> Similarly, a study on pectin aggregates<sup>18</sup> revealed that HSH can be an effective system for reducing the particle size of the pectin suspension and modifying the surface morphology and structure of the pectin. A previous study using HSH on tomato fibre revealed that HSH can modify the microstructure of fibres and alter particle size, producing products with different morphologies.<sup>17</sup> In comparison to high-pressure homogenization, HSH has the advantage of reduced energy and time consumption; therefore, investigating the effect of HSH on RCF is of both scientific and economic significance. However, to the best of our knowledge, reports on HSH-processed RCF are not available.

Considering the impact of pH-shifting on protein isolates and protein isolate extraction/preparation from the literature, we hypothesise that combining pH-shifting with high-speed homogenization will alter the structural, rheological, and functional properties of intact chia seed flour, thereby enhancing its solubility and potential for use in diverse food products. This approach provides a cost-effective and scalable alternative to protein isolate extraction, enabling the food

industry to create versatile plant-based ingredients with minimal processing.

## 2 Materials and methods

Black chia seeds (*Salvia hispanica* L.) were purchased from Royal Nut Company (Victoria, Australia), which is mentioned as a supplier from Bolivia, and were packed in Australia. Sunflower oil was purchased from MOI International (Brisbane, Australia) and stored at room temperature. Analytical grade chemicals used for this study were purchased from Sigma-Aldrich (Australia). Deionized water was used in all the experiments unless specified otherwise.

### 2.1 Chia seed flour preparation

A raw chia seed flour (RCF) suspension was prepared using simpler steps, which enhances the likelihood of commercialisation quickly. In short, chia seeds (CSs) were accurately weighed to 50 g and then further ground using a food processor (Philips HR7762/90-grinder mill, Australia) for 20 seconds. During the preliminary trials, grinding was carried out for 10 seconds, 15 seconds, 20 seconds, and 2 minutes and 30 seconds, with a 10-second break after each interval. It was observed that a longer grinding time increased the flour's clump formation due to its high oil content, and it did not easily pass through the sieves with openings of 125 microns, 180 microns, 355 microns, 500 microns, and 850 microns. Furthermore, based on the quantity of fine particles produced after grinding, it was confirmed that an 850-micron sieve with a total of 20 seconds of grinding (10 seconds of grinding, 5 seconds of break, and then 5 seconds of grinding again) yields higher efficiency. This gave 93.31 ± 0.19 (%) fine particles and 4.28 ± 0.47 (%) coarse particles, with a total recovery of 98.21 ± 0.66 (%). This flour is considered raw chia seed flour (RCF).

The particle size of RCF flour (non-hydrated) was measured using a dry dispersion unit (Refractive index 1.47, 2 bar air pressure, feed rate 100%) of a Mastersizer 2000 (Malvern Instruments, UK), according to the protocol of Badin *et al.*<sup>19</sup> The RCF used for the experiment showed  $D$  [4,3] 40.54 ± 0.48 (μm),  $D$  [3,2] 37.10 ± 0.36 (μm),  $d$  (0.1) 25.75 ± 0.44 (μm),  $d$  (0.5) 39.53 ± 0.51 (μm), and  $d$  (0.9) 56.95 ± 1.15 (μm). Previously,<sup>20</sup> the particle size of chia seed flour was measured to be  $d$  (0.1) = 23.9 ± 1.9 μm,  $d$  (0.5) = 95.3 ± 1.2 μm,  $d$  (0.9) = 181.9 ± 1.3 μm and  $D$  [4, 3] = 100.1 ± 1.1 μm. The difference in these results is due to the use of sieving. As we sifted the flour, the particle size became more uniform. However, their study found that chia seed flour contained 2 ± 1% of proteins, 30.4 ± 0.9% of fat, 8 ± 0.3% of moisture and 4.1 ± 0.8% of ash (w.b), which is different from our results due to the difference in the flour preparation method and may be due to a genetic difference in seeds. The reduced particle size can impact the functional and biological properties of chia seeds, including the digestibility of macronutrients and extractability of calcium and polyphenols.<sup>21</sup>

### 2.2 pH-Shifting of the chia seed flour suspension

RCF prepared previously (Section 2.1) was suspended in deionized water at 2% (w/w) and stirred for 15 min using an



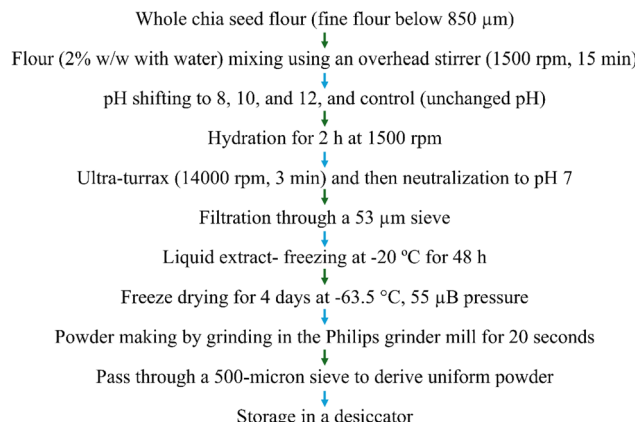


Fig. 1 Flow chart for modified chia seed flour preparation (CFs).

overhead stirrer (IKA® RW 20 digital, Germany) at 1500 rpm and room temperature ( $20 \pm 2$  °C). Furthermore, the pH of the suspension was measured using a pH meter (CUBE-121122/WHI, Australia). Initially, pH shifting was carried out using 1 M NaOH and neutralized to pH 7 using 0.5 N HCl. Ultra-turrax processing (high shear) was carried out at 14 000 rpm for 3 minutes at room temperature. Furthermore, the suspension was filtered using a 53 µm sieve (ASTM). The protocol for sample preparation is presented in Fig. 1. This ultra-turrax treatment was termed as high-speed homogenisation (HSH).<sup>17</sup>

The pictorial presentation of the modified CF preparation, from flour to liquid extracts, is shown in Fig. 2. The final freeze-dried flour was stored at  $20 \pm 2$  °C in a desiccator. Furthermore, the samples were denoted as follows: pH 8 to 7 as pH 8CF, pH 10 to 7 as pH 10CF, pH 12 to 7 as pH 12CF, the control (untreated sample) as CTCF, and raw whole chia seed flour as RCF. All the samples together are collectively referred to as chia seed flour, *i.e.*, CF, unless specified otherwise.

### 2.3 Post-processing of solid residues

The derived solid residues after filtration were subjected to oven drying at 40 °C for 24 h, further ground through the same processor for 30 seconds, and then passed through a 500 µm sieve with 100% recovery. The derived solid residue powder was stored in a desiccator until further use. The solid residues were analyzed for proximate composition.

### 2.4 Analysis of the freeze-dried functional ingredient (modified flour)

The derived freeze-dried CFs (pH 8CF, pH 10CF, pH 12CF, and CTCF) and RCF were analyzed for physical and functional properties to develop a functional ingredient. The solid residues were designated as pH 8R, pH 10R, pH 12R, and CTR, produced from the respective treated samples after pH-shifting. Together, all the residues were termed TRs (treated residues).

### 2.5 Yield, extent of extraction, and colour profile

**2.5.1 Yield.** The CF/solid residue yield was calculated with respect to the initial amount of flour taken for the modification, as in eqn (1).

$$\text{Yield}(\%) = \frac{\text{gm of freeze-dried modified flour or solid residues}}{\text{gm of initial flour}} \times 100 \quad (1)$$

**2.5.2 Extent of extraction.** The extent of extraction in terms of powdered solid residues derived from the initial flour was calculated using eqn (2).

$$\text{Extent of extraction}(\%)$$

$$= \frac{(\text{Initial flour sample} - \text{gm of oven dried solid residues})}{\text{gm of initial flour}} \times 100 \quad (2)$$

**2.5.3 Proximate composition.** The moisture, oil, and ash contents were determined using the methods outlined in the AOAC.<sup>22</sup> Protein content (C and N) was measured using a LECO macro CN828 analyzer (LECO, St. Joseph, MI, USA) by multiplying the nitrogen (%) by 6.25. Here, carbohydrate content was measured as 100 – (moisture + oil + protein + ash).<sup>23</sup>

**2.5.4 Colour profile.** In this study, colour was measured according to the protocol provided in ref. 23. The colour of CF powder or residues was analysed using a chroma meter (Konica Minolta Sensing Inc., Japan). Colour values were expressed as  $L^*$ ,  $a^*$ , and  $b^*$  in the CIE system, representing white to black, red to green, and yellow to blue, respectively. A white calibrating standard ( $L^* = 94.66$ ,  $a^* = -0.59$ ,  $b^* = 3.69$ ) was used as a reference. Chromaticity ( $C^*$ ) was calculated using eqn (3):

$$C^* = (a^{*2} + b^{*2}) \quad (3)$$

The hue angle ( $H^\circ$ ), indicating the hue of the sample, was calculated using eqn (4):

$$H^\circ = \tan^{-1}(b^*/a^*) \quad (4)$$

### 2.6 Techno-functional properties

This study subjected the CFs to analyses such as WHC, OHC, zeta potential, and solubility. Here, all the CF suspensions were prepared with water, hydrated for one hour at room temperature ( $20 \pm 2$  °C), and further allowed to stand overnight for complete absorption. During the analysis of zeta potential, particle size, rheology, and solubility, the samples were adjusted to pH 7 using 1 M NaOH and 0.5 N HCl.

**2.6.1 WHC and OHC.** WHC and OHC were determined using the protocol from ref. 12. Here, 100 mg of the sample was mixed with 1.5 g of water or oil, mixed using a vortex (2 min), and mixed using a rotary shaker for one hour at room temperature, and left overnight for absorption. Furthermore, the centrifugation was performed at 14 000×g for 10 minutes at  $27 \pm 2$  °C. The weight of the supernatant was determined, and WHC or OHC was presented as g water held per g of sample, and oil-holding capacity as g oil held per g of sample in terms of percentage<sup>12</sup> (eqn (5)).



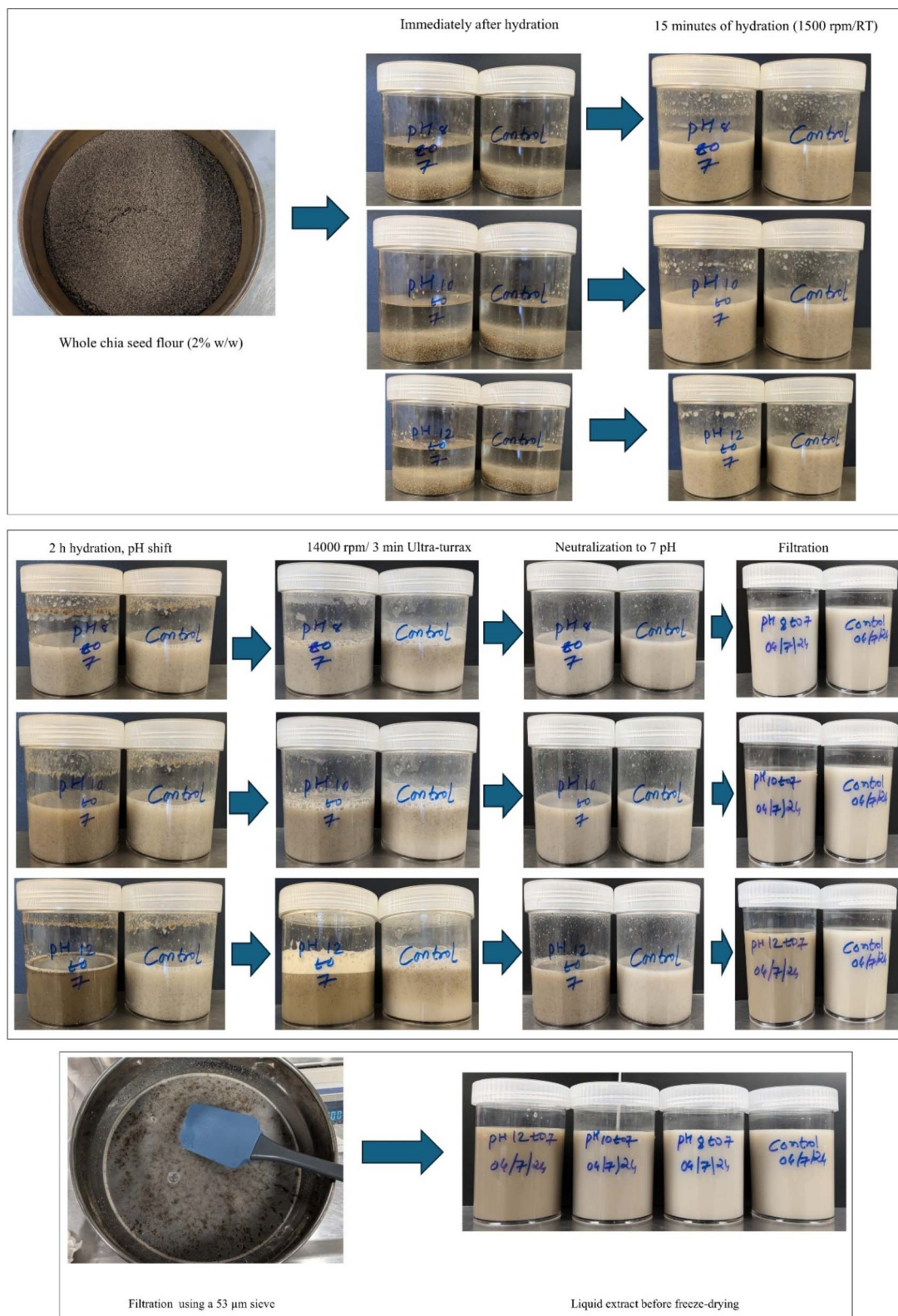


Fig. 2 Pictorial presentation of modified flour preparation.

$$\text{WHC or OHC} = \frac{H - \text{CFs}}{\text{CFs}} \times 100 \quad (5)$$

where CFs is the weight of flour, and  $H$  is the precipitate weight (g).

**2.6.2 Flour solubility.** The solubility of CFs was evaluated by suspending the samples in deionized water (1% w/w). The suspension was set to pH 7, magnetically stirred for 1 h at room temperature, kept overnight for hydration, and centrifuged at  $14\,000 \times g$  for 15 min at  $25\text{ }^\circ\text{C}$ .<sup>12</sup> The supernatant was collected, dried at  $120\text{ }^\circ\text{C}$  in an oven, and weighed until a uniform weight was found. Powder solubility (%) was measured by using the following eqn (6):

$$\text{Flour solubility} = \frac{\text{CFDs}}{\text{CFs}} \times \frac{80}{20} \times 100 \quad (6)$$

CFDs are the weight of the dried soluble fraction (g), CFs are the weight of the flour (g on a dry basis), 20 represents the ml of supernatant, and 80 represents the ml of water.

**2.6.3 Particle size.** The particle size of the dispersion was measured by modifying the protocol of ref. 24. CF dispersions were prepared (1% w/w) with deionized water, hydrated for one hour using a magnetic stirrer, and kept overnight for complete hydration at pH 7. The particle size of the dispersion was measured using a Malvern Mastersizer 2000 (Malvern Instruments Ltd, UK), with the laser obscuration being around 10–12%, and the refractive index was 1.3340 for dispersion (1% w/w) and 1.3330 for deionized water. The results were presented as the surface-weighted mean ( $[D_{3,2}]$ ), volume-weighted mean ( $[D_{4,3}]$ ),  $d$  (0.9),  $d$  (0.5), and  $d$  (0.1) determined through the instrument software.

**2.6.4 Swelling index.** The swelling index (SI) of flour was determined using the modified protocols.<sup>25,26</sup> Specifically, 0.25 g of flour sample was mixed with 5 mL of distilled water in a 10 mL measuring cylinder. The mixture was allowed to stand for 2 h before measuring the swelling level. The SI value was calculated as the volume occupied by the sample post-swelling divided by the volume occupied by the sample pre-swelling (eqn (7)).

Swelling index

$$= \frac{\text{Volume occupied by the sample after swelling}}{\text{Volume occupied by the sample before swelling}} \quad (7)$$

**2.6.5 Zeta potential.** To determine the zeta potential (ZP), a 0.1% (w/w) dispersion of the CFs was prepared by hydrating with Milli-Q water for 1 hour. Furthermore, the dispersion was kept overnight to ensure complete absorption. After that, the dispersion was centrifuged (3000 g,  $25\text{ }^\circ\text{C}$ , 30 min) to obtain a water-soluble extract (supernatant) and was further subjected to measurement of zeta potential using a folded capillary cell (DTS1060) and a Zetasizer (Malvern Zetasizer Nano ZS, UK). Zeta potential was determined from the electrophoretic mobility phenomena at  $25\text{ }^\circ\text{C}$  using a Zetasizer and presented as millivolts (mV).<sup>27</sup>

### 2.6.6 Structural (FTIR) and thermal properties (DSC)

**2.6.6.1 FTIR.** FTIR spectra of RCF, CFs, and residues were obtained using a Nicolet™ iS50 FTIR Spectrometer (Thermo Scientific, USA) to determine the structural modifications in the

functional groups. The spectra were obtained in the range of  $400\text{--}4000\text{ cm}^{-1}$  at a resolution of  $4\text{ cm}^{-1}$ , with 64 sample scans used to derive each spectrum based on absorbance.<sup>28</sup>

**2.6.6.2 DSC.** The CFs were subjected to DSC (DSC1, STAR<sup>e</sup> system, METTLER TOLEDO) to determine their thermal transition properties. A sample of 3–4 mg of each flour was accurately weighed into a  $40\text{ }\mu\text{L}$  aluminium pan and hermetically sealed. Samples were analysed from  $25\text{--}350\text{ }^\circ\text{C}$  at a heating rate of  $10\text{ }^\circ\text{C min}^{-1}$  and nitrogen flow of 20 mL per minute.<sup>29</sup>

**2.6.7 Rheology (flow behaviour).** In this study, CF dispersions were analysed for flow behaviour at a 1% (w/w) concentration and a constant temperature of  $25\text{ }^\circ\text{C}$ . A rheometer (AR-G2, TA Instruments, New Castle, DE), equipped with a parallel plate geometry (60 mm diameter, 50  $\mu\text{m}$  gap) and a Peltier element for maintaining a constant temperature, was used to determine the flow properties at  $25\text{ }^\circ\text{C}$ . A 50  $\mu\text{m}$  gap was confirmed through preliminary trials. According to the methodology of ref. 27 the flow properties were determined over a range of shear rates from 0.1 to  $100\text{ s}^{-1}$ .

**2.6.8 Statistical analysis.** All experiments were carried out in triplicate, and data are presented as mean  $\pm$  SD. One-way and two-way analysis of variance (ANOVA) was performed to test differences at a 95% ( $p < 0.05$ ) significance level, and Tukey's post hoc test was employed for multiple comparisons using OriginPRO® 2024 software. FTIR and DSC graphs were prepared using OriginPRO® 2024, while other graphs were prepared using the GraphPad Software (10.4.1).

## 3 Results and discussion

The chia seed flour was modified at pH 8, pH 10, and pH 12, along with high-speed homogenization (HSH), and the derived flour was analysed for its physicochemical and functional properties. The primary objective of this study was to investigate whether structural modifications in chia flour affect its functional properties.

### 3.1 Yield, extent of extraction, and colour profile

**3.1.1 Yield.** The yield of modified powdered chia seed flour (CFs) and solid residue was calculated based on the initial amount of flour used for sample preparation. This yield will provide a basis for calculating the extent of extraction (%). The yield of modified flour, solid residues and the extent of extraction are presented in Fig. 3. The yield of modified flour (CFs) and solid residues was significantly affected by pH shifting and HSH ( $p < 0.05$ ). The yield of modified flour (CFs) varied between 54.99% and 74.97%. pH 12CF showed the highest ( $p < 0.05$ ) yield of 74.97%, followed by 60.56% (pH 10CF), 57.64% (pH 8CF), and 54.99% (CTCF).

The increase in yield, along with the increase in pH, may be attributed to the powerful shearing of HSH, which dissolved more soluble and insoluble compounds from RCF into liquid extracts, which were then further freeze-dried to form modified flour CFs. Previously, a similar trend was observed in the preparation of the chia seed protein isolate, where the total yield increased with a pH of an alkaline medium.<sup>16</sup> It is essential



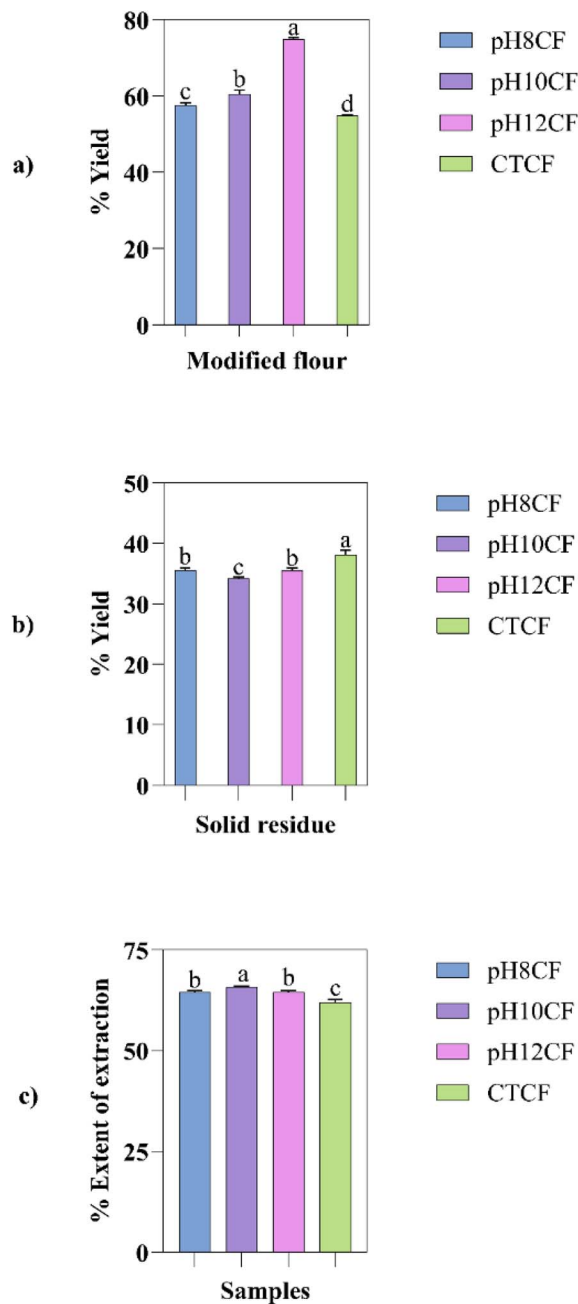


Fig. 3 Yield and extent of extraction from the shear-pH shifting treatment: (a) % yield of modified flour, (b) % yield of the solid residue, and (c) extent of extraction of samples.

to consider that HSH can increase the solid-liquid interface area, which accelerates the mass transfer kinetics between the target compound and the extractive phase (solvent).<sup>30</sup> CS, which is composed of soluble, insoluble fibres along with lignin, cellulose, and hemicellulose compounds,<sup>31,32</sup> can be affected due to the alkaline medium<sup>33</sup> which results in a higher yield of the flour with increasing pH. The yield of the solid residue was higher in CTCF, which was aligned with the observations on the yield of modified flour, where CTCF showed a lower yield. pH 10CF showed a lower yield of solid residues, and thus a higher extent of extraction as compared to pH 12CF. This may be

attributed to the compositional differences and handling losses of the derived residues. The extent of extraction increased with an increase in pH.<sup>16</sup> However, the reduction at pH 12 may be due to the hindrance created by salt formation during filtration or compositional changes.

Different superscript letters in the experiment indicate statistical significance ( $p < 0.05$ ) determined using one-way ANOVA and Tukey's post hoc test for multiple comparisons.

Thus, mechanical and chemical modifications of chia seed flour yield higher modified CFs as compared to the control.

**3.1.2 Proximate composition.** Previous studies with RCF added to bread, cake or milk products have confirmed the impact of proximate composition of chia seeds on the texture (hardness and gumminess) and total acceptable score of the final product.<sup>8,34,35</sup> Proximate composition of modified CFs and RCF, along with residues, is presented in Fig. 4(a and b).

Different superscript letters in the experiment indicate statistical significance ( $p < 0.05$ ) determined using one-way ANOVA and Tukey's post hoc test for multiple comparisons.

Overall, the composition of RCF was similar to previously reported results<sup>5,10,23</sup> including moisture (7.13%), oil (35.61%), ash (4.45%), carbohydrates (32.27%), and protein (20.54%), as shown in Fig. 4(b).

For the treated samples, moisture (4.04–4.25%), oil (30.93–48.51%), protein (21.46–27.33%), carbohydrate (14.85–18.82%), and ash contents were observed to be between 5.28% and

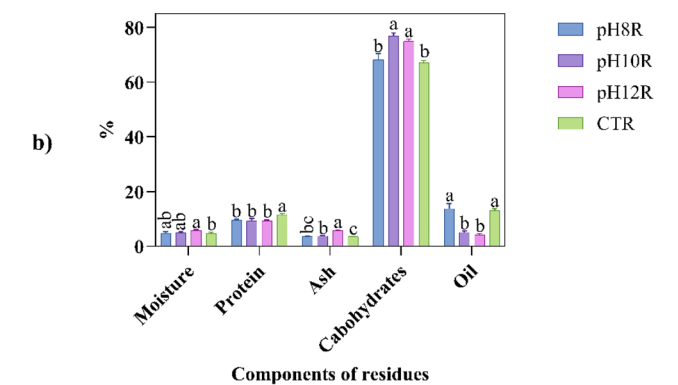
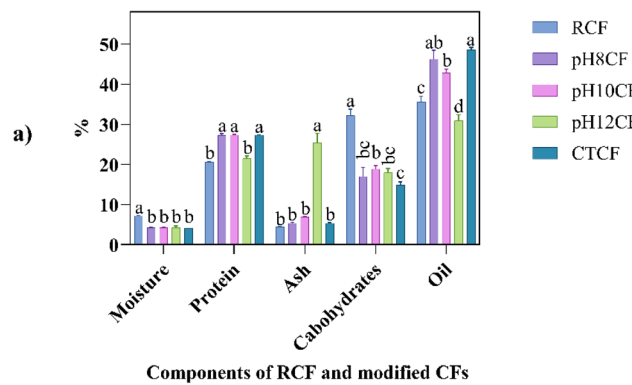


Fig. 4 Proximate composition: (a) RCF and modified CFs and (b) residues.

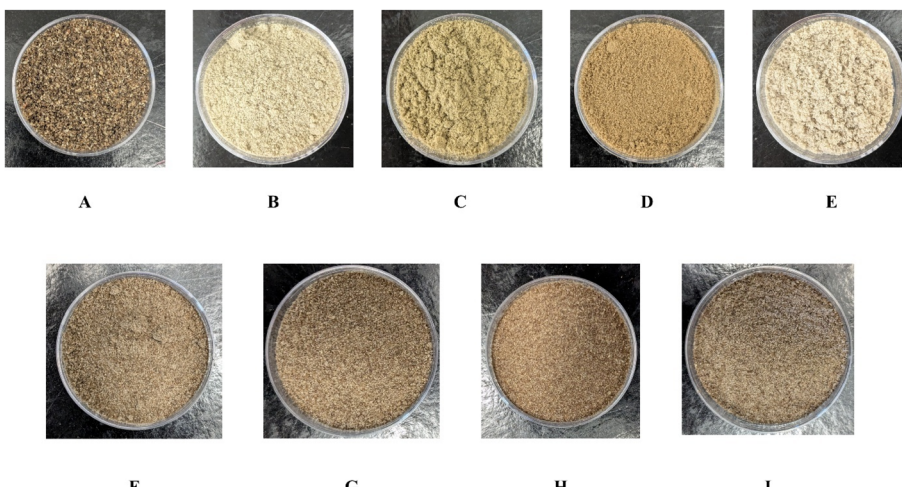


Fig. 5 RCF, modified chia seed flour, and solid residues derived from the alkaline-shear approach: (A) RCF, (B) pH 8CF, (C) pH 10CF, (D) pH 12CF, (E) CTCF, (F) pH 8R, (G) pH 10R, (H) pH 12R, and (I) CTR.

25.47%. pH 8CF, pH 10CF, pH 12CF, and CTCF showed non-significant results for moisture content, while variations were observed for oil, protein, carbohydrate, and ash contents. It was observed that at pH 12, the ash content significantly ( $p < 0.05$ ) increased, which may be attributed to the solubilization of more compounds (minerals), salts developed during the neutralisation, and some absorbed material, which helped to increase the ash content.<sup>33</sup> Reduction of protein and fat content was observed in the study of ref. 33 where defatted flour of Rambutan (*Nephelium lappaceum*) was treated at pH 8–9 for 4 h. Protein content in this modified CF was found to be closer to the protein content of the fibrous fraction of chia seed (28.14  $\pm$  0.36%),<sup>36</sup> and 26.0  $\pm$  0.9 (%).<sup>10</sup>

The reduction in carbohydrate content in treated samples (pH 8CF, pH 10CF, pH 12CF, and CTCF) may be attributed to the fractionation process, which involves sieving and HSH, where insoluble compounds are filtered using a sieve. CTCF has lower carbohydrate content ( $p < 0.05$ ) compared to pH 10CF, due to the alkaline medium. The increased oil content in treated samples compared to RCF may be accompanied by a reduction in total solid mass, particularly in carbohydrates, and an impact of HSH and a higher mixing speed (1500 rpm, 2 min), which further breaks the walls of the chia seed and extracts more oil. Previously, a study on CPI preparation observed a reduction in the oil content after applying alkaline treatment,<sup>16</sup> which contradicts our findings, possibly due to HSH. The saponification reaction can occur at a pH of 12, potentially affecting the functional properties and storage stability of modified flour.

However, it's also crucial to examine how the alkaline approach affects specific ingredients, such as fibre, protein, and oil. The increase in particle size of the processed samples (Section 3.2.1) suggests that mucilage may serve as an emulsifier and antioxidant, preserving the oil during HSH treatment by regulating saponification. However, the system may become even more stable under pH-shear circumstances if additional antioxidants are included. According to a recent review on

protein–polysaccharide interactions, pH is considered an extrinsic factor that affects the interactions between these polymers.<sup>37</sup> pH influences the stability of the complexes and determines how a polymer interacts with other polymers and with the surrounding solvent. Changes in pH can alter the density of polysaccharides (affecting network formation) and influence the net charge on proteins. Under high pH conditions (above the isoelectric point), a stable dispersion can occur due to electrostatic repulsion between the negatively charged polysaccharides and protein. On the other hand, under low pH conditions, protein–polysaccharide complexes can form through electrostatic attraction between positively charged proteins and negatively charged polysaccharides. These pH-driven changes regulate the characteristics of the complexes and nano/microparticles, influencing their charge, size, interactions, system stability and rheological properties based on the concentrations of polymers. The pH-dependent interactions between proteins and polysaccharides can influence the stability and strength of the complex and can also alter the type and nature of the interaction, affecting the overall structure and properties of the protein–polysaccharide complex. However, these interactions can enhance the functional properties of the complexes; they can also be influenced by other factors, including the presence of salt.<sup>37</sup>

For the residues, moisture (4.70–5.81%), oil (4.13–13.78%), protein (9.25–11.59%), carbohydrate (67.11–76.95%), and ash contents were observed to be between 3.51% and 5.81%. Like modified CFs, higher ash content was observed in pH 12R, which may be due to the absorbed material (salt formation) during the neutralisation of the liquid extract. The higher protein content in CTR may be due to protein accumulation, which is not soluble in water at pH 6.13 (the pH of RCF + water). However, alkaline-treated samples (pH 8CF, pH 10CF, and pH 12CF) showed lower protein content in the residues ( $p < 0.05$ ). More carbohydrates were observed in pH 10R and in pH 12R. This may be due to the impact of pH, where structural carbohydrates located on the vegetable cellular wall could be



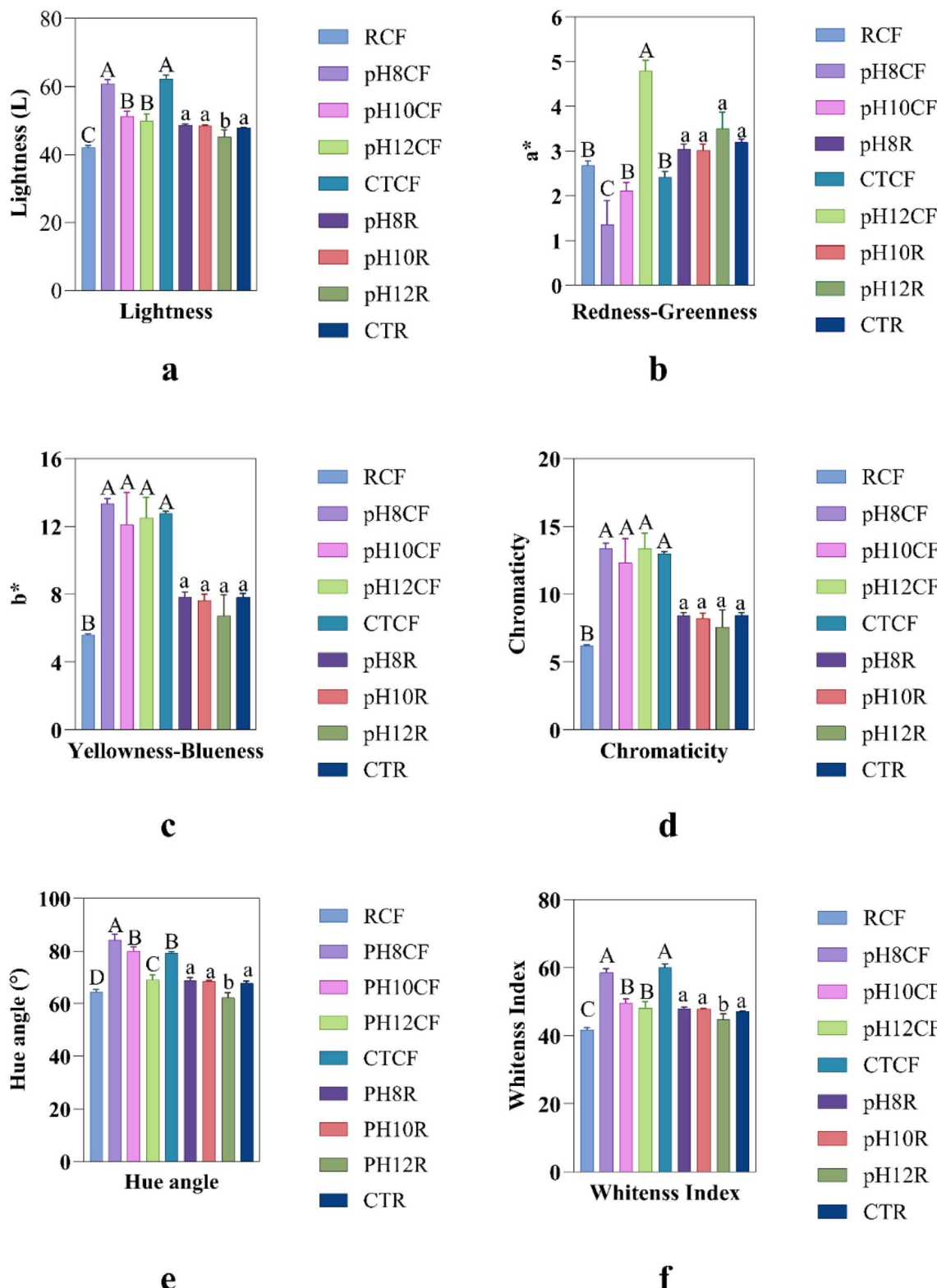


Fig. 6 Colour profile of modified chia seed flour and residues: (a) lightness ( $L^*$ ), (b) redness-greenness ( $a^*$ ), (c) yellowness-blueness ( $b^*$ ), (d) chromaticity, (e) hue angle, and (f) whiteness index.

retained, and only cellular components could be transferred.<sup>38</sup> Since the protein and oil contents were higher in the modified flour, the functional properties were characterised only for the

flour, and composition, colour profile, and FTIR analyses were performed for the residues.

**3.1.3 Colour profile.** CS and RCF are used in various baked products, dairy products, meat and fish products, gluten-free

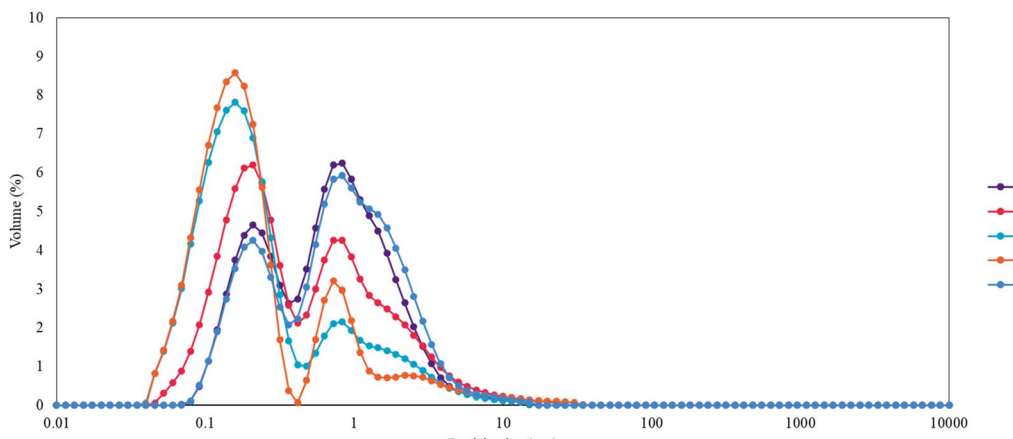


Fig. 7 Particle size distribution of modified chia seed flour (pH 8CF, pH 10CF, pH 12CF, and CTCF) and raw chia seed flour (RCF).

products, and other products.<sup>5</sup> However, the addition of whole chia seed flour, or defatted chia seed flour can reduce the lightness of the food product.<sup>8,39–42</sup> Thus, this chia seed flour can be unacceptable for use at a higher rate in the product. Thus, there is a scope for improving the colour of chia seed flour. Thus, this study formulated modified CFs with better lightness, which is visible in Fig. 5. However, the solid residues seem identical in visual appearance.

The colour profiles of the RCF, modified chia seed flour, and solid residues are presented in Fig. 6. The lightness ( $L^*$ ) of RCF was observed to be  $42.12 \pm 0.60$ , which was further significantly ( $p < 0.05$ ) increased upon treating with HSH (CTCF:  $62.31 \pm 1.08$ ), and pH-HSH (pH 8CF:  $60.87 \pm 1.23$ ). The reduced lightness ( $p < 0.05$ ) in pH 10CF and pH 12CF may be due to the extraction of natural pigments and polyphenolic compounds at alkaline pH.<sup>14</sup> This may also be attributed to the oxidation of these polyphenolic compounds.<sup>14,43,44</sup> The lightness of pH 8CF and CTCF was found to be superior to that of the samples (pH 10CF and pH 12CF), which may be attributed to the minimal pH. These values were also found to be in accordance with the results of the whiteness index, as shown in Fig. 6.

The redness/greenness ( $a^*$ ), yellowness/blueness ( $b^*$ ), chromaticity, and hue angle ( $H^\circ$ ) were also affected by the processing conditions. The highest redness/greenness ( $a^*$ ) values of pH 12CF ( $a^*: 4.79 \pm 0.24$ ) can be attributed to the impact of alkaline treatment and HSH, where higher pH causes the extraction of natural pigments. However, the  $b^*$  value was found to be

equivalent ( $p > 0.05$ ) in modified flour (CFs) but higher ( $p < 0.05$ ) than that of the RCF. The results of chromaticity were found to be increased ( $p < 0.05$ ) after treatment compared to RCF. This suggests that greater colour intensity can be perceived by humans, as zero corresponds to neutral colours (grey shades), whereas 60 indicates live colours, considering a quantitative colour attribute used to determine the degree of difference of a shade compared with a grey colour of the same lightness.<sup>45</sup> The hue angle ( $H^\circ$ ) of RCF is found to be lower than that of the modified flour, which suggests that the treatment has improved the colour profile of the modified flour.

Different superscript uppercase letters in the experiment indicate statistical significance ( $p < 0.05$ ) determined using one-way ANOVA and Tukey's post hoc test for multiple comparisons. The different superscript lowercase letters in the experiment indicate statistical significance ( $p < 0.05$ ) determined using one-way ANOVA and Tukey's post hoc test for multiple comparisons.

**3.1.4 Colour profile of solid residues.** Solid residues' lightness ( $L^*$ ) ranged between  $45.31 \pm 1.90$  and  $48.74 \pm 0.28$ . The colour of pH 12R ( $45.31 \pm 1.90$ ) showed a lower lightness than that of other samples (Fig. 6), which may be due to the impact of natural pigments or phenolic compounds, as well as the effects of alkaline extraction followed by oven drying. The whiteness index also showed similar trends. In this study, the  $a^*$  value ranged between  $3.01 \pm 0.15$  and  $3.50 \pm 0.37$ , while the  $b^*$  value varied between  $6.73 \pm 1.22$  and  $7.85 \pm 0.26$ . These were  $a^*$ ,  $b^*$ , and chromaticity, which were non-significant ( $7.59 \pm 1.25$  to  $8.46 \pm$

Table 1 Particle size of RCF and modified CF dispersions (1% w/w)<sup>a</sup>

Sample	$D [4, 3]$ – volume weighted mean	$D [3, 2]$ – surface weighted mean	$d (0.1)$	$d (0.5)$	$d (0.9)$
RCF	$0.919 \pm 0.023^b$	$0.381 \pm 0.045^a$	$0.158 \pm 0.013^a$	$0.633 \pm 0.079^a$	$1.915 \pm 0.030^b$
pH 8CF	$0.872 \pm 0.048^b$	$0.238 \pm 0.004^b$	$0.108 \pm 0.002^b$	$0.315 \pm 0.004^b$	$1.994 \pm 0.009^b$
pH 10CF	$0.535 \pm 0.052^c$	$0.149 \pm 0.002^c$	$0.076 \pm 0.000^c$	$0.171 \pm 0.002^c$	$1.342 \pm 0.106^c$
pH 12CF	$0.642 \pm 0.043^c$	$0.144 \pm 0.005^c$	$0.075 \pm 0.002^c$	$0.162 \pm 0.005^c$	$1.045 \pm 0.037^d$
CTCF	$1.056 \pm 0.057^a$	$0.404 \pm 0.019^a$	$0.159 \pm 0.003^a$	$0.715 \pm 0.046^a$	$2.233 \pm 0.097^a$

<sup>a</sup> Here, values are presented as mean  $\pm$  SD. Different letters in the columns indicate significant differences ( $p < 0.05$ ) as determined through one-way ANOVA and Tukey's test.



0.20). The hue angle ( $H^\circ$ ) varied between  $62.29 \pm 1.91$  and  $68.82 \pm 1.07$  ( $H^\circ$ ). pH 12 showed a reduced hue angle, which may be due to alkaline extraction and the impact of oven drying ( $40^\circ\text{C}$ , 24 h), which formed a yellow tinge in pH 12R. The residues were not further used for other analysis, but X-ray diffraction can be studied to understand the impact of processing on the crystalline and amorphous structure of the samples.

### 3.2 Techno-functional properties

**3.2.1 Particle size.** The particle size distribution of modified chia seed flour derived from alkaline-HSH, along with untreated RCF, is presented in Fig. 7, and the volume-weighted mean and surface-weighted mean of particles are presented in Table 1.

The RCF dispersion (1% w/w) has comparatively smaller particles (below 2  $\mu\text{m}$ ) than what has been reported previously,<sup>12</sup> where partially defatted chia fibre–protein concentrate showed the main population of 200  $\mu\text{m}$  particles with a broad population peak of small particles. This difference may be due to the varying composition, hydration process, concentration of dispersions, and particle size of raw chia seed flour. Previously, a study on flaxseed confirmed that grinding can influence the particle aggregate and geometry.<sup>46</sup>

In our study, a bimodal distribution with a wide peak of larger particles was observed for the RCF and CTCF, which aligns with the observations in ref. 12, where the distribution shifted to monomodal after applying a homogenization treatment with high-pressure (100 and 150 MPa, 1, 3, and 5 passes). The pH shifting (pH 10CF and pH 12CF) increased the population of smaller particles, resulting in a slight movement to the left with a steeper distribution, which follows a similar pattern of high-pressure homogenization, and HSH, along with the increased passes.<sup>12,47</sup> It can be considered that pH-shifting supports the fragmentation of large particles into smaller ones, forming a more homogeneous dispersion due to the mechanical shear of the HSH process.<sup>17</sup> Additionally, the alkaline treatment may reduce the viscosity of the liquid after HSH, which supports the reduction of larger particles during filtration, forming a dispersion with smaller particles than those of pH 8CF, CTCF, and RCF.

Previously, a study on tomato fibre,<sup>17</sup> where HSH and acidic conditions were applied, revealed that acidic conditions, along with HSH, promoted the reduction in particle size, which we expect to occur in the case of chia seed. The alkaline conditions may have helped dissolve the insoluble portion of the chia seed flour into a partially soluble fraction, along with vigorous HSH, which reduced the particle size of the filtered, freeze-dried, modified flour. Previously, a study confirmed the reduction of hemicellulose, cellulose and lignin from the plant matrix (cocksfoot grass) upon alkaline treatment using NaOH and KOH.<sup>48</sup> Probably, the increased specific surface area improved the diffusion of compounds, along with violent shearing, which may have intensified molecular collisions and increased the hydrolysis of the particles, potentially reducing the particle size of pH 10 and pH 12 CF.

The particle size of CTCF was observed to be higher than that of RCF (Fig. 7) which may be attributed to the formation of large aggregates upon extensive hydration at 1500 rpm for 2 h without

the alkaline treatment, which may support the swelling of chia seed mucilage, mechanical treatment (HSH) that may have helped to enclose the larger particles within the swelled mucilage of flour, agglomeration of smaller particles, and compositional difference between RCF and CTCF. As chia seed contains soluble and insoluble fibre, it may be possible that CTCF changed the structure and percentage of fibres (water-soluble and insoluble) of particles during the treatment. These structural changes could affect the functional properties of modified chia seed flour. A previous study using partially defatted chia seed flour revealed that high-pressure homogenization can alter the percentage of total dietary fibre, resulting in a reduction of insoluble dietary fibre and an increase in soluble dietary fibre.<sup>12</sup> To support this hypothesis, the water holding capacity (WHC), oil holding capacity (OHC), solubility, and rheological properties of the dispersion were analysed in the later sections.

**3.2.2 WHC and OHC.** WHC and OHC of modified CFs, along with RCF, are reported in Fig. 8. WHC was significantly ( $p < 0.05$ ) lower for pH-shifting-HSH-treated samples compared to RCF ( $5.55 \pm 0.06 \text{ g g}^{-1}$ ) (Fig. 8(a)). The OHC is higher for the treated sample compared to the RCF (Fig. 8(b)).

Different superscript letters in the experiment indicate statistical significance ( $p < 0.05$ ) determined using one-way ANOVA and Tukey's post hoc test for multiple comparisons.

Previous studies identified that the higher WHC of RCF may be due to the presence of chia seed mucilage,<sup>36</sup> total dietary fibre

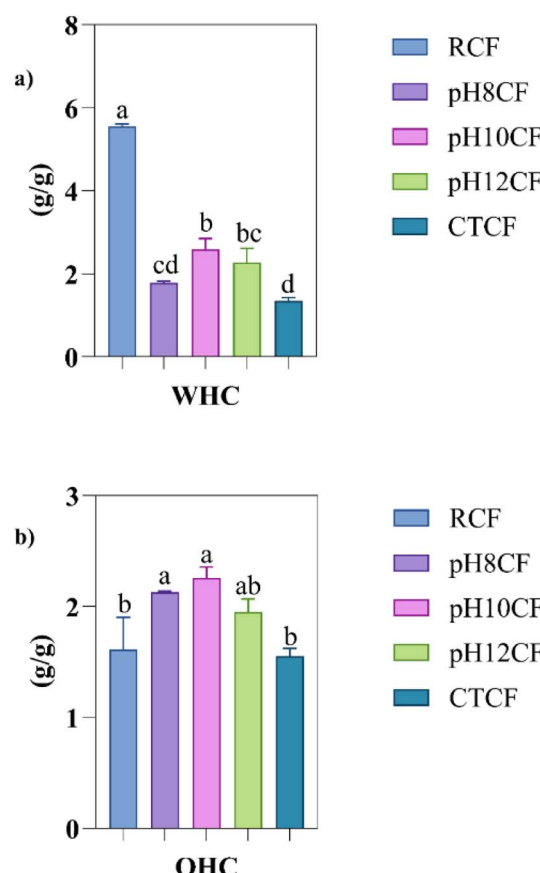


Fig. 8 WHC and OHC of modified CFs: (a) WHC and (b) OHC.

(soluble and insoluble components), or polysaccharides and non-polysaccharide compounds in the fibre.<sup>12,31,38</sup> Also, the hydrophilic chains of the fibre and proteins contribute to the water retention capacity.<sup>49</sup> The reduced WHC in treated samples may be attributed to the fractionation carried out *via* sieving, HSH<sup>12</sup> and alkaline treatment. This can also be due to changes in the structural modifications of both insoluble and mucilaginous soluble fibres, as well as the exposure of hydrophobic protein residues, which can affect WHC more significantly.

The OHC depends upon the surface properties of particles (available area and hydrophobicity).<sup>12,50</sup> OHC of RCF ( $1.61 \pm 0.29 \text{ g g}^{-1}$ ) was observed to be significantly ( $p < 0.05$ ) lower than that of pH 8CF ( $2.13 \pm 0.01 \text{ g g}^{-1}$ ) and pH 10CF ( $2.26 \pm 0.10 \text{ g g}^{-1}$ ). However, pH 8CF, pH 10CF, and pH 12CF showed equivalent ( $p > 0.05$ ) OHC. The increased OHC in treated samples as compared to RCF may be attributed to the reduced particle size of modified flour<sup>36</sup> or its composition. Also, the chemical treatment enhanced the lipophilic behaviour of CFs. However, the OHC observed in this study was closer to the values reported in previous studies on various chia seed fractions, such as fibre-rich fraction ( $2.02 \text{ g g}^{-1}$ ),<sup>36</sup> chia seed flour ( $1.46 \pm 0.17 \text{ g g}^{-1}$ ),<sup>51</sup> deoiled chia seed meal (solvent meal ( $2.03 \pm 0.08 \text{ g g}^{-1}$ )), solvent fibre-rich fraction ( $2.06 \pm 0.03 \text{ g g}^{-1}$ ), pressing meal ( $1.26 \pm 0.03 \text{ g g}^{-1}$ ), and pressing fibre-rich fraction ( $1.40 \pm 0.18 \text{ g g}^{-1}$ ).<sup>38</sup>

The high-pressure homogenization was carried out in ref. 12 on partially defatted chia fibre–protein concentrate (24.7% protein, 56.0% dietary fibre, and 9.0% fat), confirming the impact of homogenization on reduced particle size and WHC, which can form dietary fibre-rich ingredients with reduced WHC, and is particularly interesting to avoid competition for water between fibre and gluten proteins, which reflects on dough development. According to Alfredo *et al.*,<sup>36</sup> the fibre-rich fraction, with low OHC, around  $2.02 \text{ g g}^{-1}$ , can be used as a potential ingredient in fired products, as it provides a non-greasy sensation.

**3.2.3 Swelling index (SI).** The ability to form the gel of chia seed flour depends on the flour's swelling index (SI) and solubility. These determine the interaction of water with flour,<sup>11</sup> which measures the flour's ability to absorb water and swell. The SI of RCF and modified CFs was calculated as the volume occupied by the sample post-swelling divided by the volume occupied pre-swelling. RCF showed the highest ( $p < 0.05$ ) swelling index among all the tested samples, of  $2.93 \pm 0.12$  (SI), while pH 8CF showed the lowest SI ( $1.21 \pm 0.02$ ). Furthermore, pH 12CF ( $1.79 \pm 0.13$ ) and pH 10CF ( $1.45 \pm 0.34$ ) exhibited an equivalent ( $p > 0.05$ ) SI, while CTCF ( $1.28 \pm 0.13$ ), pH 8CF and pH 10CF presented an equivalent SI. The highest SI in RCF is attributed to the CSM (high content of fibres),<sup>49</sup> which swelled and acquired more volume after being immersed in water. These results are closer to the report on quinoa flour (germinated and high-pressure homogenised) ( $1.18\text{--}1.60$ ),<sup>25</sup> and amaranth flour (1.02%).<sup>26</sup> Furthermore, the pH 12CF and pH 10CF showed equivalent results, which matched the trend of WHC, suggesting the impact of smaller particle size and pH treatment with HSH. This may be attributed to the dissolution of more soluble mucilage and breakdown of other compounds

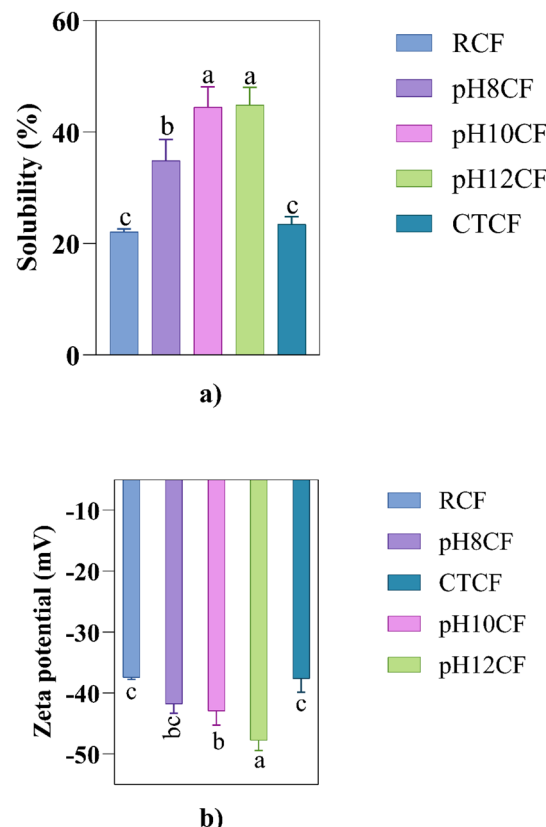


Fig. 9 (a) Solubility and (b) zeta potential of chia seed flour samples.

(fibres) during shearing through HSH. pH 8CF, pH 10CF and CTCF showed equivalent results, which may be due to the lower content of soluble fibres. According to ref. 52, the swelling capacity of flour depends on particle size, processing or unit operations. Previously ref. 49, showed that high fibre content can contribute to the swelling capacity of chia seed flour, but proteins also enhance the retention of water and subsequent swelling occurs. Thus, it increases the volume gain from the absorption of water. Previously, the swelling capacity of chia seed flour was reported to be  $11.82 \pm 1.12 \text{ (mL g}^{-1})$ ,<sup>49</sup>  $4.62 \pm 0.92 \text{ (g g}^{-1})$ ,<sup>53</sup>  $7.46 \pm 1.00 \text{ (g g}^{-1})$ ,<sup>51</sup> and  $19.74 \pm 0.95 \text{ (g g}^{-1})$ .<sup>11</sup> This difference between our results and the literature can be due to the difference in flour sample (composition and particle size) used and the protocol followed, as this includes the use of a centrifuge to remove the supernatant, which measured the SI with respect to the sample, weight of residues, and dried supernatant. The reduced swelling index of modified CFs can be useful for food products where a firmer, less sticky texture is desired.

**3.2.4 Flour solubility.** Solubility of modified chia seed flour and RCF is presented in Fig. 9(a). RCF showed an overall solubility of  $22.06 \pm 0.56\%$ , which was found to be higher compared to the previous work on chia seed flour (8.79–15.5%),<sup>51,54</sup> which may be due to the different composition of raw chia seed flour, milling technique, and the particle size of the non-hydrated flour. Modified CFs such as pH 8CF ( $34.89 \pm 3.79\%$ ), pH 10CF ( $44.55 \pm 3.53\%$ ), and pH 12CF ( $44.88 \pm 3.16\%$ ) showed higher



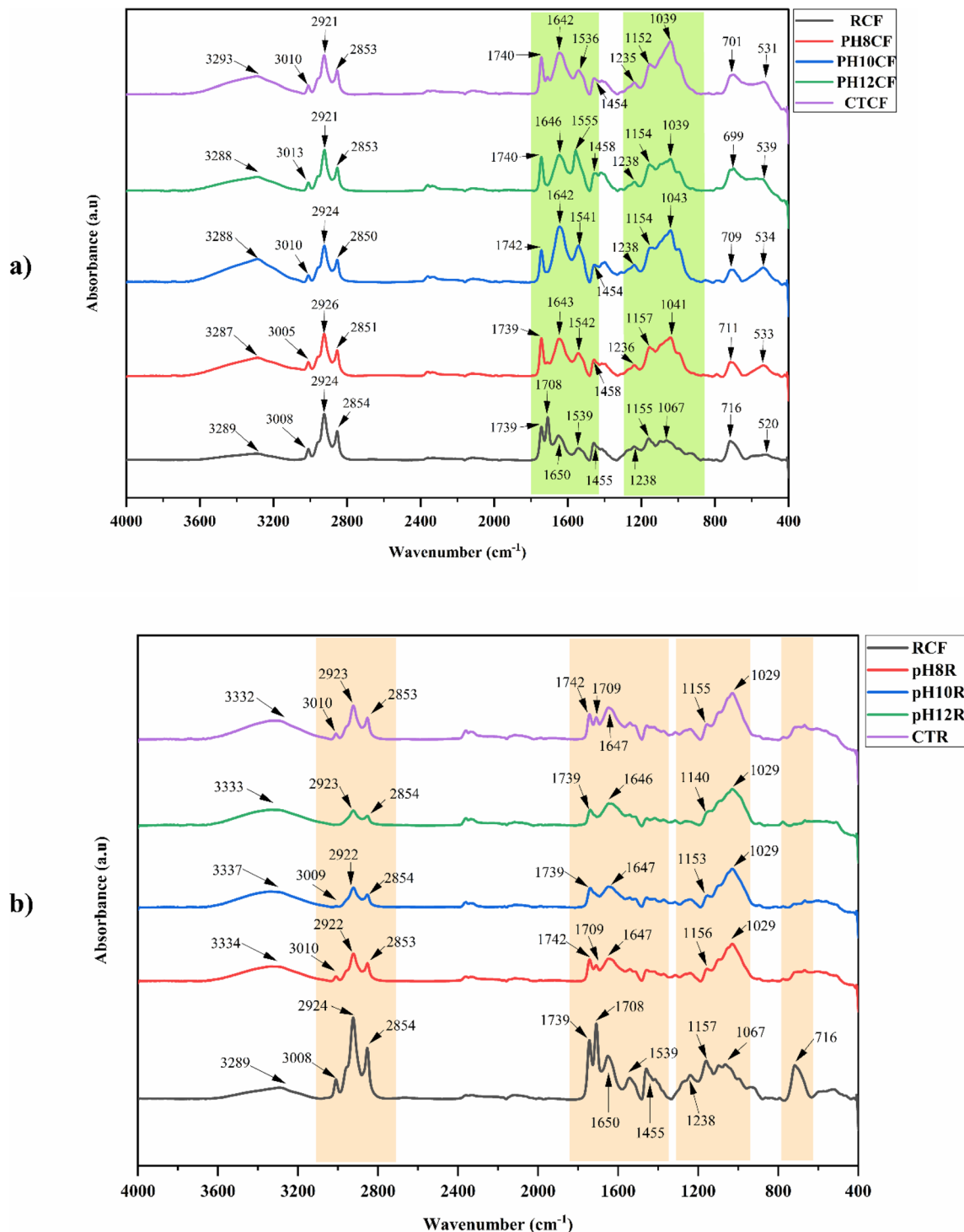


Fig. 10 FTIR analysis of samples: (a) RCF and modified flour, and (b) RCF and residues.

solubility ( $p < 0.05$ ) as compared to RCF and CTCF ( $23.47 \pm 1.37\%$ ). This may be linked to the redistribution of fibre components from insoluble to soluble fractions under alkaline-HSH conditions, the disintegration of insoluble fibre during mechanical treatment (HSH), and the structure of flour particles. Also, there may be changes in the exposed groups of proteins that can form hydrogen bonds with water, leading to enhanced solubility.<sup>12</sup>

Since particle size decreased, the surface areas of the chia seed flour particles increased, so that interactions between water and flour were enhanced, leading to increased solubility.<sup>12</sup>

Different superscript letters in the experiment indicate statistical significance ( $p < 0.05$ ) determined using one-way ANOVA and Tukey's post hoc test for multiple comparisons.

**3.2.5 Zeta potential.** One of the most crucial aspects of proteins and polysaccharides is their  $\zeta$ -potential, also known as

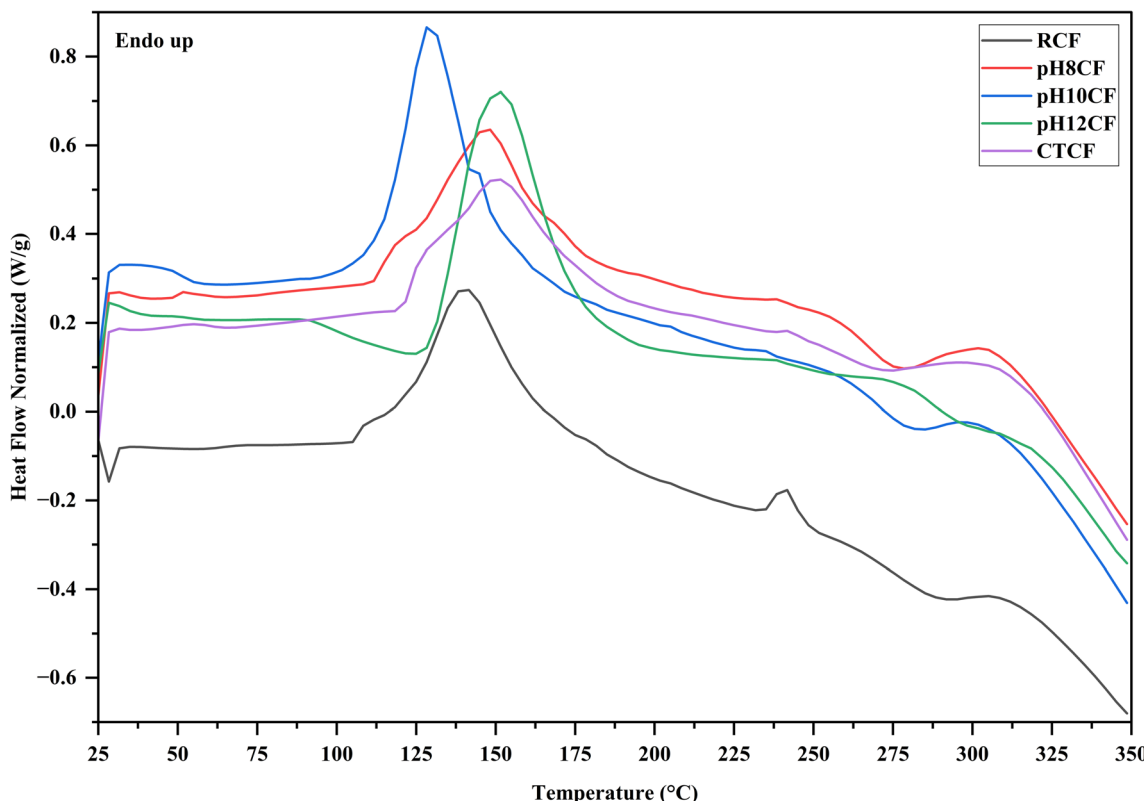


Fig. 11 Thermal analysis of RCF and modified CFs.

surface charge, which affects their solubility and functional properties, such as their ability to emulsify and foam. The degree of interaction between colloidal particles is mostly determined by the surface charge. The degree of attraction or repulsion between the adjacent charged colloids is likewise reflected in the  $\zeta$  potential.<sup>55,56</sup> States that in general, a value outside the range of  $-30$  to  $+30$  mV is thought to have enough repulsive forces to achieve satisfactory physical colloidal stability. At the same time, van der Waals forces may cause particle aggregation if ZP is modest. The medium's pH is one of the main elements influencing the ZP. As a result, ZP of all the samples was examined at pH 7.0 and is presented in Fig. 9(b).

RCF showed  $(-37.47 \pm 0.31$  mV) equivalent ( $p > 0.05$ )  $\zeta$ -potential with CTCF  $(-37.67 \pm 2.20$  mV), but a lower value compared to pH 8CF  $(-41.80 \pm 1.51$  mV), pH 10CF  $(-42.97 \pm 2.31$  mV), and pH 12CF  $(-47.80 \pm 1.68$  mV). The higher absolute value of zeta potential increased under alkaline conditions (Fig. 9(b)). This may be due to the solubilization of soluble fibre (mucilage-polar in nature)<sup>29,57</sup> of chia seed at an alkaline pH. Solubility of chia seed proteins and zeta potentials also increased along with increased pH,<sup>58</sup> which may be the reason for the dissolution of more soluble proteins in the modified CFs. However, the study from ref. 59 showed that, when the pH is higher than the isoelectric point of chia seed proteins, the carboxyl groups ( $-\text{COO}^-$ ) outnumber the amino groups ( $\text{NH}^{3+}$ ), leading to the net negative charge in the protein.

The increased repulsive force among similarly charged molecules decreases the probability of protein molecule

aggregation and reduces the air bubbles' coalescence. The increase in net charge not only increases the solubility but also increases the proteins' surface activity and flexibility, allowing them to spread more quickly on the air-water interface, entrapping air bubbles and thus increasing foam formation.<sup>58</sup>

### 3.3 Structural and thermal properties

**3.3.1 FTIR.** The FTIR spectrum provides information about the chemical groups and their vibrational state, which is related to changes in the chemical composition of the raw material after a process, without destroying the samples.<sup>49</sup> FTIR analysis of modified flour and residues in comparison with RCF is presented in Fig. 10(a) and (b), respectively.

The figures showed the FTIR spectrum from 400 to  $4000\text{ cm}^{-1}$ , marking the critical changes with colours. Since the modified flours were prepared after hydrating the RCF, CSM, and other soluble compounds, these may impact the overall FTIR spectrum of the modified CFs. All the samples exhibited a similar pattern, but some characteristic changes were observed in the intensity and the breadth of the peaks (Fig. 10(a and b)), which may be attributed to the process of pH shifting and HSH. The characteristic peak near  $3300\text{ cm}^{-1}$  could be attributed to the OH group stretching,<sup>12,49</sup> and some N-H stretching of proteins coupled with a hydrogen bond.<sup>60</sup> The peak observed at around  $3008\text{ cm}^{-1}$  is attributed to the *cis*-type unsaturated CH group ( $\text{C}=\text{C}-\text{H}$  stretching).<sup>49,61</sup> The peak near 2921 may be attributed to C-H stretching.<sup>12,61</sup> Around



Table 2 Thermal transition in RCF and modified CFs<sup>a</sup>

Thermal transition	RCF	pH 8CF	pH 10CF	pH 12CF	CTCF
<b>Peak 1 (endothermic)</b>					
$T_o$ (°C)	58.07 ± 4.88 <sup>a</sup>	46.98 ± 4.82 <sup>ab</sup>	37.21 ± 2.35 <sup>b</sup>	40.07 ± 4.48 <sup>b</sup>	45.37 ± 2.27 <sup>ab</sup>
$T_p$ (°C)	70.31 ± 1.22 <sup>a</sup>	50.72 ± 0.81 <sup>b</sup>	44.38 ± 5.08 <sup>b</sup>	46.97 ± 3.72 <sup>b</sup>	56.13 ± 0.95 <sup>b</sup>
Enthalpy (J g <sup>-1</sup> )	0.28 ± 0.04 <sup>a</sup>	0.20 ± 0.06 <sup>a</sup>	0.31 ± 0.23 <sup>a</sup>	0.24 ± 0.18 <sup>a</sup>	0.47 ± 0.25 <sup>a</sup>
$T_e$ (°C)	81.31 ± 0.86 <sup>a</sup>	55.99 ± 3.53 <sup>b</sup>	51.53 ± 2.33 <sup>b</sup>	53.06 ± 5.72 <sup>b</sup>	63.92 ± 0.88 <sup>b</sup>
<b>Peak 2 (endothermic)</b>					
$T_o$ (°C)	116.95 ± 3.08 <sup>a</sup>	114.54 ± 3.03 <sup>a</sup>	117.20 ± 2.14 <sup>a</sup>	126.63 ± 6.72 <sup>a</sup>	120.92 ± 0.26 <sup>a</sup>
$T_p$ (°C)	139.21 ± 1.70 <sup>ab</sup>	147.05 ± 0.45 <sup>ab</sup>	132.68 ± 5.20 <sup>b</sup>	151.35 ± 0.46 <sup>a</sup>	145.39 ± 6.58 <sup>ab</sup>
Enthalpy (J g <sup>-1</sup> )	83.30 ± 6.45 <sup>ab</sup>	62.77 ± 1.80 <sup>b</sup>	86.45 ± 4.62 <sup>ab</sup>	124.22 ± 27.24 <sup>a</sup>	70.81 ± 0.96 <sup>b</sup>
$T_e$ (°C)	167.02 ± 0.76 <sup>ab</sup>	172.14 ± 6.80 <sup>ab</sup>	151.66 ± 5.87 <sup>b</sup>	177.08 ± 1.17 <sup>a</sup>	172.57 ± 10.10 <sup>ab</sup>
<b>Peak 3 (endothermic)</b>					
$T_o$ (°C)	233.46 ± 2.47 <sup>a</sup>	234.00 ± 1.46 <sup>a</sup>	229.76 ± 0.44 <sup>a</sup>	233.62 ± 0.36 <sup>a</sup>	235.37 ± 2.31 <sup>a</sup>
$T_p$ (°C)	239.14 ± 2.22 <sup>a</sup>	240.10 ± 1.41 <sup>a</sup>	233.74 ± 0.68 <sup>a</sup>	237.30 ± 0.71 <sup>a</sup>	239.21 ± 3.85 <sup>a</sup>
Enthalpy (J g <sup>-1</sup> )	3.76 ± 0.56 <sup>a</sup>	0.80 ± 0.46 <sup>b</sup>	0.25 ± 0.06 <sup>b</sup>	0.19 ± 0.02 <sup>b</sup>	0.36 ± 0.06 <sup>b</sup>
$T_e$ (°C)	246.06 ± 2.26 <sup>a</sup>	246.40 ± 4.76 <sup>a</sup>	237.63 ± 0.13 <sup>a</sup>	241.79 ± 1.40 <sup>a</sup>	244.31 ± 3.31 <sup>a</sup>
<b>Peak 4 (exothermic)</b>					
$T_o$ (°C)	268.03 ± 0.01 <sup>b</sup>	260.75 ± 1.86 <sup>bc</sup>	262.47 ± 2.55 <sup>bc</sup>	281.85 ± 1.16 <sup>a</sup>	254.40 ± 3.62 <sup>c</sup>
$T_p$ (°C)	286.82 ± 0.93 <sup>b</sup>	276.79 ± 0.93 <sup>c</sup>	278.51 ± 1.46 <sup>c</sup>	295.92 ± 0.11 <sup>a</sup>	272.32 ± 1.22 <sup>d</sup>
Enthalpy (J g <sup>-1</sup> )	-5.62 ± 0.62 <sup>a</sup>	-7.53 ± 2.89 <sup>a</sup>	-9.34 ± 3.60 <sup>a</sup>	-3.80 ± 2.70 <sup>a</sup>	-5.92 ± 0.09 <sup>a</sup>
$T_e$ (°C)	302.75 ± 1.15 <sup>b</sup>	290.51 ± 3.08 <sup>c</sup>	294.56 ± 2.24 <sup>bc</sup>	313.34 ± 3.71 <sup>a</sup>	292.68 ± 0.25 <sup>c</sup>

<sup>a</sup> Here  $T_o$ : onset temperature;  $T_p$ : peak temperature;  $T_e$ : end set temperature;  $P_t$ : peak time (minutes). Here, values are presented as mean ± SD, different letters in the row indicate significant differences ( $p < 0.05$ ) as determined using Tukey's test for a particular peak number.

1740 cm<sup>-1</sup>, the peak observed may be attributed to C=O stretching (carboxyl groups),<sup>49,61</sup> which seems to show equivalent intensity for CTCF and pH 8CF. According to ref. 62, peaks observed at 1743, 2854, and 2924 cm<sup>-1</sup> were also attributed to the lipid profile of chia seeds. Also, the changes in the carbohydrate composition and protein/lipid changes may be attributed to the peaks at 1740–1750 cm<sup>-1</sup> and 2800–3000 cm<sup>-1</sup>, respectively.<sup>54</sup> We suspect that pH-HSH may have changed the unsaturated and saturated fat compositions of modified CFs. Additionally, the peak near 1708 cm<sup>-1</sup>, which was sharper, was reduced in pH 8CF and CTCF, while completely disappearing in pH 10CF and pH 12CF due to alkaline/HSH treatment.

The peak observed at around 1642–1650 cm<sup>-1</sup> could be assigned to C=O stretching and the amide-I group (secondary structure), which showed major changes in intensity, with pH 10CF exhibiting higher intensity while RCF showed lower intensity. This may be linked to the changes in the protein structure of CS resulting from processing. While 1517–1550 cm<sup>-1</sup> represents the amide II regions for chia seed proteins,<sup>63</sup> the amide II region (N–H bending/C–N stretching of proteins) observed in ref. 60 near 1551 cm<sup>-1</sup> for partially defatted flour with 35% protein content, was found to be closer to that in our study in RCF, but the peak showed higher intensity for pH 10CF and pH 12CF, suggesting the impact of the alkaline medium on the proteins, while pH 8CF and CTCF showed similar intensity, showing similar functional properties.<sup>63</sup>

Previously, a study showed that the use of alkaline conditions (pH 10 and pH 12) may affect the structure of chia seed protein isolates.<sup>15</sup> The stretching of the carboxyl group (–COO–)

of uronic acids may be the reason for the peaks observed at around 1500 and 1454–1458 cm<sup>-1</sup>.<sup>29,61</sup> However, a weak peak at 1456 cm<sup>-1</sup> may also be attributed to –N=N=O, related to the proteins.<sup>49</sup> The peak found at 1235–1238 cm<sup>-1</sup> was attributed to the presence of amide III.<sup>54</sup> The peak observed at 1039–1067 cm<sup>-1</sup> could correspond to the stretching vibrations of the pyranose ring.<sup>49,61</sup>

Major changes were also observed at 1200–1251 cm<sup>-1</sup> (Fig. 10(a)), which are responsible for the changes in the structure of proteins (β-sheet)<sup>15</sup> in modified flours. It was also reported that slight changes in the wavenumber of chia seed proteins may result from differences in functional groups, amino acid composition, and interactions among them when alkaline (pH 10 and pH 12) conditions were applied to isolate proteins.<sup>15</sup> Also, the gradual unfolding of the protein tertiary structure was observed when extracted at higher alkaline pH.<sup>15</sup>

Further changes at 1000–1100 cm<sup>-1</sup> may be attributed to the changes in glycosidic bonding (pyranose ring) in the flour (CSM fraction of flour), which may be attributed to changes in the carbohydrates.<sup>29,49</sup> The peak orientation observed at 1000–1100 cm<sup>-1</sup> for RCF appears distinct from that of the modified flour, which may be attributed to the influence of CSM extraction and other water-soluble compounds resulting from the pH-HSH treatment. The changes observed at 750–1200 cm<sup>-1</sup> may also be attributed to the changes in lipid release, changes in proteins, and changes in the fingerprint region of carbohydrates.<sup>62</sup> The peak near 699 cm<sup>-1</sup> may be attributed to aromatic C–C groups,<sup>62</sup> which are found to be different in RCF and modified CFs.



Overall, the changes observed in OH stretching (peaks at around  $3300\text{ cm}^{-1}$ ), C–H stretching ( $2950\text{--}2850\text{ cm}^{-1}$ ), and  $1600\text{ cm}^{-1}$  ( $\text{C}=\text{O}$  stretching) might be due to the changes observed in the phenolic compounds, and changes in the lipid profile of the chia after the treatment.<sup>61,62</sup> Changes in the protein structure may be attributed to changes in the intensity of peaks and variations in peak shape (broad or sharp peaks) at  $1200\text{--}1800$ .<sup>15,54,63</sup> It is interesting to study the impact of processing on the structure of proteins in detail and the lipid profile of oils in the modified flour.

For the residues (Fig. 10(b)), the intensity difference and changes in the peaks (Fig. 10(b)) were studied, revealing the impact of the process and the leaching of soluble compounds into the liquid after filtration. Interestingly, most of the peaks showed higher intensity in the RCF, suggesting the presence of an abundance of those functional groups (compounds) in the samples. This confirms that pH shifting-HSH and filtration have altered the functional groups of residues and modified CFs at the molecular level as well.

**3.3.2 DSC.** The thermal analysis of RCF and modified CFs was carried out to understand the thermal behaviour of the flour. Fig. 11 provides the thermal transition of samples (RCF and modified CFs). Overall, four peaks were observed for all the samples, from which three peaks showed the endothermic transition, and one showed the exothermic reactions presented in Fig. 11.

In general, the endothermic peaks are related to the loss of moisture (free water) from the sample, the removal of bound water, or the denaturation of proteins if the sample is composed of proteins and polysaccharides,<sup>15,29</sup> while the exothermic peaks represent decomposition or oxidative degradation. Interestingly, pH 12CF showed higher moisture levels while the control had the lowest, which matched the trend of energy for peak 2. Previous reports have provided the thermal transition for partially defatted chia seed flour, protein isolates, or protein-rich fractions; however, they have not provided the thermal transition for chia seed flour alone without hydration. This work first defined the changes in chia seed flour without hydration under a controlled temperature increase. Overall, for the partial defatted chia seed flour, the denaturation range is  $66.4\text{--}152.72\text{ }^\circ\text{C}$ , which is closely aligned with the range of the second peak of endothermic reactions. The denaturation enthalpy for the partially defatted chia seed flour was  $151.4\text{ J g}^{-1}$ ,<sup>60</sup> which differed from our results and may be due to differences in composition. The changes observed in endothermic peak 2, where a higher energy is required for pH 12CF, may be attributed to differences in protein content, ash content, and the endothermic nature of hydrophobic interactions.<sup>60</sup> The higher the energy of the peak, the more stable the structure of proteins and other compounds. pH 10CF and pH 12CF exhibited a higher magnitude for the endothermic reaction (peak 2) (Table 2), which may be attributed to the uniform dimension of powder aligning with the observations for corn and barley protein concentrates, where micronised and fine particles showed higher enthalpy for endothermic reactions. A more uniform structural distribution of the molecules leads to a more cooperative phase transition, resulting in a more intense phenomenon.<sup>64</sup> These observations aligned with the results of

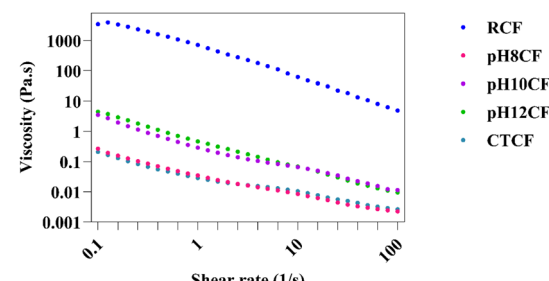


Fig. 12 Flow behaviour of CFs for the 1% (w/w) dispersion (pH 7).

the particle size analysis as well. The changes in endothermic reactions also depend on the amount of a particular fraction of protein present (albumins, globulins, prolamins, and glutelins in the samples), as all the fractions have different denaturation temperatures and enthalpy requirements.<sup>65</sup>

The decomposition temperature (peak temperature of the exothermic peak) of pH 12CF was found to be higher than that of other samples, suggesting the impact of extensive alkaline pH-HSH, which may have contributed to increasing the temperature of decomposition or oxidative degradation of polysaccharides or other soluble compounds under alkaline conditions. However, a deeper understanding can be developed about the impact of pH-HSH on the individual components (protein, fibre, and oil) of chia seed flour and their thermal characteristics.

### 3.4 Flow behaviour of flour

The flow behaviour of CFs was determined for the 1% (w/w) dispersion (pH 7) at shear rates of  $0.1\text{ to }100\text{ S}^{-1}$  (at  $25\text{ }^\circ\text{C}$ ) and is presented in Fig. 12.

RCF and modified CFs showed shear-thinning behaviour,<sup>49</sup> which can be due to the pseudoplastic nature of dispersions as observed with chia seed mucilage<sup>23</sup> or breaking protein–protein interactions between the proteins' chains due to the applied deformation.<sup>32</sup>

RCF showed higher viscosity,  $3477.33 \pm 131.07\text{ (Pa s)}$  at  $0.1\text{ (S}^{-1}\text{)}$ , which was around 700 times higher than that of pH 12CF ( $4.47 \pm 0.91\text{ Pa s}$ ) and 900 times higher than that of pH 10CF ( $3.53 \pm 0.31\text{ Pa s}$ ). pH 10 and pH 12CF showed nearly equivalent flow behaviour, which may be attributed to the composition of these fluids. This reduction in viscosity is attributed to HSH, which reduces the particle size, apparently affects the carbohydrate content of modified CFs (as shown in the proximate composition), and disrupts the gel structure during HSH. However, the viscosities of pH 8CF and CTCF were comparatively lower, at  $0.27 \pm 0.03\text{ (Pa s)}$  and  $0.21 \pm 0.02\text{ (Pa s)}$ , respectively. This may be attributed to the less solubilization of soluble fibres and other fibres from flour to liquid samples during the processing. Higher viscosity of RCF had impaired the properties of many products, such as gluten-free rice layer cake,<sup>42</sup> pound cake,<sup>9</sup> tofu<sup>66</sup> and bread.<sup>8</sup> Thus, it is interesting to use modified CFs with higher oil and protein contents and lower viscosity in the preparation of leavened bakery products.



## 4 Conclusion

The raw chia seed flour was subjected to alkaline-shear technology (pH-HSH) to produce a modified ingredient that can be used in moderately viscous food products, offering a better colour profile and improved functional properties. pH-HSH has affected the colour profile and functional properties of modified chia seed flour. The yield of modified flour is affected by the increase in alkaline conditions. Furthermore, the colour profile of pH 8CF and CTCF was improved compared to that of RCF, which may broaden its application in various food products. Alkaline-HSH affected the particle size, which reduced with an increase in pH and increased the solubility of modified flour. Furthermore, the zeta potential exhibited more negative values, which aligned with the hypothesis that more soluble compounds would be extracted in an alkaline medium. Reduced WHC of modified flour can be used in leavened cereal products. Significant reduction in apparent viscosity suggests the use of modified CFs in various leavened bakery products, where the texture of the final product is very important. DSC and FTIR supported the hypothesis of molecular modification in chia seed flour. Thus, this pH-HSH-based modification can be an approach to modify the RCF for wide use in various products where the use of chia seed is limited.

This work was solely focused on flour and changes that occurred in the flour, so in the future, it is interesting to study the impact of pH-HSH on phenolic compounds, flavonoids, and type of oil (omega-3 or omega-6 fatty acids), and changes that appear in the protein profiling of chia seed proteins and oils under thermal transition. The impact of processing on individual components can be studied. Additionally, there may be a chance of saponification of the oil through alkaline treatment. This can be further compared with deoiled flour with a similar approach to study the changes in the functional properties of flour. The addition of plant extracts that have antioxidative potential and aromatic compounds can be another option to enhance the use of modified chia seed flour in various products. This study suggests that the pH-HSH treatment is a promising approach for modifying chia seed flour, providing a scalable and cost-effective method to enhance its functional and structural properties. For industrial applications, future pilot-scale studies should assess processing efficiency, the stability of modified chia flour during storage (including its functional properties), compatibility with existing food manufacturing systems, and its performance in real food matrices, such as beverages, drinks, baked goods, and plant-based formulations.

## Conflicts of interest

All the authors declare that there is no conflict of interest.

## Data availability

Data will be made available on request.

## References

- 1 F. Valenzuela Zamudio, R. Rojas Herrera and M. R. Segura Campos, *Curr. Opin. Food Sci.*, 2024, **57**, 101149.
- 2 Z.-u. Din, M. Alam, H. Ullah, D. Shi, B. Xu, H. Li and C. Xiao, *Food Hydrocolloids Health*, 2021, **1**, 100010.
- 3 S. Biswas, F. Islam, A. Imran, T. Zahoor, R. Noreen, M. Fatima, S. M. Zahra and M. Asif Shah, *Cogent Food Agric.*, 2023, **9**, 2220516.
- 4 D. Solanki, N. Hans, J. K. Sahu, B. Bhandari, S. Prakash and S. Hati, *Innov. Food Sci. Emerg. Technol.*, 2025, **104**, 104157.
- 5 V. Zettel and B. Hitzmann, *Trends Food Sci. Technol.*, 2018, **80**, 43–50.
- 6 C. de Souza Paglarini, G. de Figueiredo Furtado, A. R. Honório, L. Mokarzel, V. A. da Silva Vidal, A. P. B. Ribeiro, R. L. Cunha and M. A. R. Pollonio, *Food Struct.*, 2019, **20**, 100105.
- 7 C. Senna, L. Soares, M. B. Egea and S. S. Fernandes, *Molecules*, 2024, **29**, 440.
- 8 M. S. Coelho and M. D. L. M. Salas-Mellado, *LWT-Food Sci. Technol.*, 2015, **60**, 729–736.
- 9 P. Luna Pizarro, E. L. Almeida, N. C. Sammán and Y. K. Chang, *LWT-Food Sci. Technol.*, 2013, **54**, 73–79.
- 10 A. Alonso-Álvarez and C. M. Haros, *Eur. Food Res. Technol.*, 2025, **251**, 3793–3806.
- 11 S. Ramos, P. Fradinho, P. Mata and A. Raymundo, *J. Sci. Food Agric.*, 2017, **97**, 1753–1760.
- 12 N. Renoldi, S. Melchior, S. Calligaris and D. Peressini, *Food Hydrocolloids*, 2023, **139**, 108505.
- 13 L. Wu, J. Li, W. Wu, L. Wang, F. Qin and W. Xie, *J. Cereal. Sci.*, 2021, **101**, 103314.
- 14 D. N. López, R. Ingrassia, P. Busti, J. Wagner, V. Boeris and D. Spelzini, *LWT-Food Sci. Technol.*, 2018, **97**, 523–529.
- 15 D. N. López, R. Ingrassia, P. Busti, J. Bonino, J. F. Delgado, J. Wagner, V. Boeris and D. Spelzini, *LWT-Food Sci. Technol.*, 2018, **90**, 396–402.
- 16 E. S. I. Khushairay, M. A. A. Ghani, A. S. Babji and S. M. Yusop, *Foods*, 2023, **12**, 3046.
- 17 X. Hua, S. Xu, M. Wang, Y. Chen, H. Yang and R. Yang, *Food Chem.*, 2017, **232**, 443–449.
- 18 J. Chen, S.-S. Wu, R.-H. Liang, W. Liu, C.-M. Liu, X.-X. Shuai and Z.-J. Wang, *Food Chem.*, 2014, **165**, 1–8.
- 19 R. Badin, C. Gaiani, S. Desobry, S. Prakash, B. Bhandari, R. Rasch, H. Bostelmann and J. Burgain, *Carbohydr. Polym.*, 2025, **350**, 123057.
- 20 S. Verdú, F. Vásquez, E. Ivorra, A. J. Sánchez, J. M. Barat and R. Grau, *J. Cereal. Sci.*, 2015, **65**, 67–73.
- 21 J. Calvo-Lerma, C. Paz-Yépez, A. Asensio-Grau, A. Heredia and A. Andrés, *Foods*, 2020, **9**, 290.
- 22 W. Horwitz, *Official Methods of Analysis of AOAC International. Volume I, Agricultural Chemicals, Contaminants, Drugs*, ed. W. Horwitz, AOAC International 1997., Gaithersburg (Maryland), 2010.
- 23 D. Solanki, P. Dhungana, Q. Y. Tan, R. Badin, B. Bhandari, J. K. Sahu and S. Prakash, *Food Hydrocolloids*, 2024, **110342**, DOI: [10.1016/j.foodhyd.2024.110342](https://doi.org/10.1016/j.foodhyd.2024.110342).



24 K. Rawal, P. K. Annamalai, B. Bhandari and S. Prakash, *J. Food Eng.*, 2023, **340**, 111300.

25 D. Thakur, M. A. Bareen, J. K. Sahu and S. Saha, *Food Hydrocolloids*, 2024, **155**, 110172.

26 A. Malik, K. Khamrui and W. Prasad, *Future Foods*, 2021, **3**, 100027.

27 Á. J. Pastrana-Pastrana, A. C. Flores-Gallegos, D. F. Roa-Acosta, R. Rodríguez-Herrera and J. F. Solanilla-Duque, *Food Hydrocolloids*, 2025, **158**, 110457.

28 L. A. Silva, P. Sinnecker, A. A. Cavalari, A. C. K. Sato and F. A. Perrechil, *Food Chem. Adv.*, 2022, **1**, 100024.

29 Y. P. Timilsena, R. Adhikari, S. Kasapis and B. Adhikari, *Carbohydr. Polym.*, 2016, **136**, 128–136.

30 R. W. S. dos Santos, L. C. Freitas, M. L. Corazza, R. C. da Silva, M. R. Mafra and T. L. P. Dantas, *Chem. Eng. Process. Process. Intensif.*, 2025, **207**, 110081.

31 M. I. Capitani, S. M. Nolasco and M. C. Tomás, *Food Ind.*, 2013, **19**, 421–437.

32 E. Averina, J. Konnerth, S. D'Amico and H. W. G. van Herwijnen, *Ind. Crops Prod.*, 2021, **161**, 113187.

33 J. Eiamwat, S. Wanlapa and S. Kampruengdet, *Molecules*, 2016, **21**, 364.

34 D. Romankiewicz, W. H. Hassoon, G. Cacak-Pietrzak, M. Sobczyk, M. Wirkowska-Wojdyła, A. Ceglińska and D. Dziki, *J. Food Qual.*, 2017, **2017**, 7352631.

35 M. E. Eker and S. Karakaya, *Int. J. Gastron. Food Sci.*, 2020, **22**, 100276.

36 V.-O. Alfredo, R.-R. Gabriel, C.-G. Luis and B.-A. David, *LWT-Food Sci. Technol.*, 2009, **42**, 168–173.

37 A. Babu, R. Shams, K. K. Dash, A. M. Shaikh and B. Kovács, *J. Agric. Food Res.*, 2024, **18**, 101510.

38 M. I. Capitani, V. Spotorno, S. M. Nolasco and M. C. Tomás, *LWT-Food Sci. Technol.*, 2012, **45**, 94–102.

39 S. Chemutai, M. Mburu, D. Njoroge and V. Zettel, *Foods*, 2024, **13**, 543.

40 V. da Costa Borges, S. S. Fernandes, E. da Rosa Zavareze, C. M. Haros, C. P. Hernandez, A. R. Guerra Dias and M. de las Mercedes Salas-Mellado, *Food Biosci.*, 2021, **43**, 101294.

41 E. N. Guiotto, M. C. Tomás and C. M. Haros, *Foods*, 2020, **9**, 819.

42 W. C. Sung, E. T. Chiu, A. Sun and H. I. Hsiao, *J. Food Sci.*, 2020, **85**, 545–555.

43 B. Salcedo-Chávez, J. A. Osuna-Castro, F. Guevara-Lara, J. Domínguez-Domínguez and O. Paredes-López, *J. Agric. Food Chem.*, 2002, **50**, 6515–6520.

44 M. E. Steffolani, P. Villacorta, E. R. Morales-Soriano, R. Repetto-Carrasco, A. E. León and G. T. Pérez, *Cereal Chem.*, 2016, **93**, 275–281.

45 F. S. D. Santos, R. M. F. D. Figueirêdo, A. J. de Melo Queiroz, Y. F. Paiva, A. C. D. Araújo, T. L. B. D. Lima, A. J. de Brito Araújo Carvalho, M. dos Santos Lima, A. D. B. D. Macedo and A. R. N. Campos, *J. Therm. Anal. Calorim.*, 2023, 1–13.

46 D. Lascano, D. Garcia-Garcia, S. Rojas-Lema, L. Quiles-Carrillo, R. Balart and T. Boronat, *Appl. Sci.*, 2020, **10**, 3688.

47 D. Su, X. Zhu, Y. Wang, D. Li and L. Wang, *LWT-Food Sci. Technol.*, 2019, **116**, 108573.

48 S.-F. Sun, H.-Y. Yang, J. Yang and Z.-J. Shi, *Ind. Crops Prod.*, 2022, **178**, 114654.

49 Á. J. García-Salcedo, O. L. Torres-Vargas, A. del Real, B. Contreras-Jiménez and M. E. Rodriguez-Garcia, *Food Struct.*, 2018, **16**, 59–66.

50 G. López, G. Ros, F. Rincón, M. Periago, M. Martínez and J. Ortuno, *J. Agric. Food Chem.*, 1996, **44**, 2773–2778.

51 N. Mollakhalili-meybodi, N. Jamali, M. Sharifian, M. Kiani and A. Nematollahi, *Appl. Food Res.*, 2024, **4**, 100517.

52 S. Chandra, S. Singh and D. Kumari, *J. Food Sci. Technol.*, 2015, **52**, 3681–3688.

53 E. A. Otondi, J. M. Nduko and M. Omwamba, *J. Agric. Food Res.*, 2020, **2**, 100058.

54 M. Hatamian, M. Noshad, S. Abdanan-Mehdizadeh and H. Barzegar, *NFS J.*, 2020, **21**, 1–8.

55 K. Shevkani, N. Singh, J. C. Rana and A. Kaur, *Int. J. Food Sci. Technol.*, 2014, **49**, 541–550.

56 R. J. Hunter, *Zeta Potential in Colloid Science: Principles and Applications*, Academic Press, London, 1981.

57 L. A. Muñoz, A. Cobos, O. Diaz and J. M. Aguilera, *J. Food Eng.*, 2012, **108**, 216–224.

58 Y. P. Timilsena, R. Adhikari, C. J. Barrow and B. Adhikari, *Food Chem.*, 2016, **212**, 648–656.

59 Y. P. Timilsena, B. Wang, R. Adhikari and B. Adhikari, *Food Hydrocolloids*, 2016, **52**, 554–563.

60 M. S. Coelho and M. D. I. M. Salas-Mellado, *LWT-Food Sci. Technol.*, 2018, **96**, 26–33.

61 M. Laçin and A. Başman, *Food Sci. Nutr.*, 2025, **13**, e70308.

62 A. Kataria, S. Sharma, A. Singh and B. Singh, *J. Food Meas. Char.*, 2022, **16**, 332–343.

63 S. Dirr, O. O. Karslioglu, E. G. Ates and M. H. Ozturk, *Future Foods*, 2025, 100729, DOI: [10.1016/j.fufo.2025.100729](https://doi.org/10.1016/j.fufo.2025.100729).

64 P. Conte, M. Paciulli, M. Mefleh and F. Boukid, *Eur. Food Res. Technol.*, 2024, **250**, 2363–2373.

65 B. L. Olivos-Lugo, M. Á. Valdivia-López and A. Tecante, *Food Sci. Technol. Int.*, 2010, **16**, 89–96.

66 K.-C. Hsieh, T.-C. Lin and M.-I. Kuo, *LWT-Food Sci. Technol.*, 2022, **154**, 112676.

